

# We are IntechOpen, the world's leading publisher of Open Access books Built by scientists, for scientists

5,600

Open access books available

137,000

International authors and editors

170M

Downloads

Our authors are among the

154

Countries delivered to

TOP 1%

most cited scientists

12.2%

Contributors from top 500 universities



WEB OF SCIENCE™

Selection of our books indexed in the Book Citation Index  
in Web of Science™ Core Collection (BKCI)

Interested in publishing with us?  
Contact [book.department@intechopen.com](mailto:book.department@intechopen.com)

Numbers displayed above are based on latest data collected.  
For more information visit [www.intechopen.com](http://www.intechopen.com)



# New Approach Measuring the Wheel/Rail Interaction Loads

*Yuri P. Boronenko, Rustam V. Rahimov and Waail M. Lafta*

## Abstract

This chapter suggested new methods for monitoring the dynamic processes of rolling stock/rail interaction. This study develops a new technical solution for measuring the wheel/rail interaction forces on a significant part of the sleeper. The theoretical part of this study, using FEM, confirm the ability of piecewise continuous recording of vertical and lateral forces from the wheel/rail interaction by measuring the stresses in two sections of the rail. Also, the optimum location of strain gauges and the effective length of the measuring zone have been determined. The experimental part of this study has been carried out on the stands and the railway track to confirm the effectiveness of the method to determine the vertical and lateral wheel/rail interaction forces, increase the reliable statistical data, improve the measurement accuracy, reducing the time and cost compared with current testing methods. The developed method is recommended to determine the wheel/rail interaction forces and identify defects on the wheels when diagnosing rolling stock on operational and travel regimes.

**Keywords:** wheel/rail interaction, rolling stock/track effects, vertical force and lateral force of rolling stock, rail strain gauge, effective rail zone, wheel/rail loads

## 1. Introduction

The rapid development of heavy traffic is one of the priorities to increase the efficiency of rail transportation, which allows the formation of freight trains of increased weight and length. However, this will increase axle loads and issues related to controlling rolling stock/rail interaction forces.

The first experimental assessments of the force impact of rolling stock on a rail track were carried out in the late 19th and early 20th centuries [1–3]. In 1925, an experimental method on the rolling stock/rail impact was developed, the forces acting on the track, stresses, and deformations in the track elements have been investigated [4]. Direct measurement of the wheel/rail interacting forces is difficult; therefore, their determination is usually carried out indirectly by measuring shear deformations, and relative displacements using strain gauges and the subsequent application of algorithms for processing the data obtained [5–9].

Early research confirmed that since the maximum stresses arise at the edges of the rail base, the vertical and lateral forces have been initially determined from their correlation dependencies on the half-sum and half-difference of edge stresses [7, 10]. Later, these studies were developed in the works of M.F. Verigo, O.P. Ershkova [11], S.S. Krepkorosky, A.K. Shafranovsky [12, 13] and others [14–16].

The main disadvantage of this method is that the received results depend on the elastic properties of the path [4]; therefore, the error ratio reaches 30% [7].

E.M. Bromberg and O.P. Ershkov were developed, theoretically substantiated and practically implemented a more accurate experimental method for measuring vertical and lateral forces (“three-point” method) [11, 17] by simultaneously registering stresses at three points, **Figure 1**), measuring stresses at the edges of the rail base (strain gauges 1 and 2) and in the outer section of the headrail (strain gauge 3) [7, 14, 15, 18].

The absence of computers (during that period) limited the development of the “three-point” method. Subsequently, the method was replaced by the analog Schlumpf method [19–21] for measuring the rolling stock force effect on the rail. According to this method, the lateral forces are measured by the deformations of the rail web by four strain gauges (numbers 6–9 in **Figure 1**). The essence of this method lies in the linear dependence of the magnitude of the lateral forces on the difference in bending moments acting on points mutually symmetric to the neutral axis of the rail neck [7, 14, 22].

Researches revealed that the shortage of the Schlumpf method [22, 23] is inaccurate results on the measurement of wheel/rail interaction forces when the acting point of the vertical force displace relative to the longitudinal plane of the rail due to the lateral displacement of the wheelset in the track. The values of the lateral forces in the wheel/rail contact depend on the position of the contact spot on the railhead; therefore, errors are inevitable in determining their values. According to VNIIZhT research [14], the greatest error in measuring lateral forces by this method is 7–9%; according to the VNIKTI results [22], the method can error up to 40%. While, according to the VNICTT research [24], the error can reach 100%. Subsequently, Schlumpf’s method was improved and modernized by many researchers, to which a significant number of theoretical and experimental studies are devoted, for example, G.F. Agafonova [25], E.I. Danilenko [26], V.S. Kossova [27], A.K. Shafranovsky [12, 13] and other sources [15, 22, 25, 27].

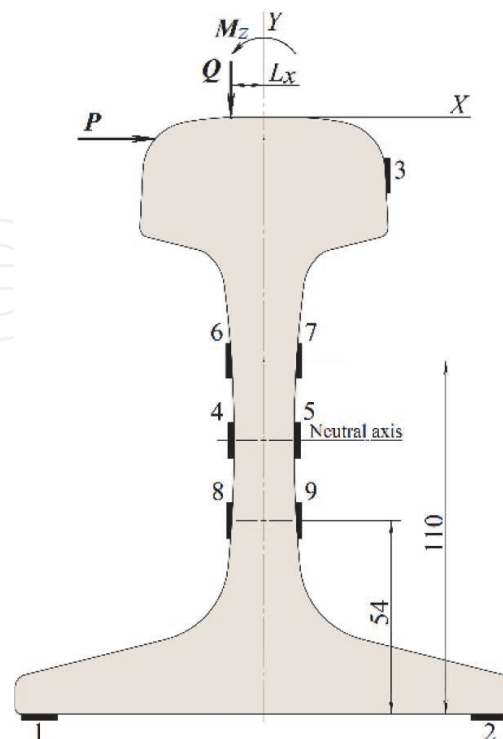


**Figure 1.** Schemes of sticking strain gauges on the rail neck to determine the rolling stock/rail force: 1–9 - strain gauge numbers;  $Q$  is the vertical force;  $P$  - lateral force;  $M_z$  - bending moment;  $X$ ,  $Y$  - directions of the axes of the coordinate system.

To determine the vertical forces in the wheel/rail contact, a method based on the measurement of deformations by using strain gauges (#4 and #5 in **Figure 1**), installed vertically from both sides in the same section on the neutral axis of the rail journal, is widely used [3, 6, 7]. This method for measuring vertical forces depends on the lateral force and the eccentricity of the vertical force [4].

For the correct measurement of the wheel/rail interaction forces, an experimental and computational method [27] have been developed to install strain gauges, similar to the Schlumpf method. This method's difference lies in the joint measurement of the vertical and lateral forces in the cross-section of the rail at different positions of the wheel on the rail [22–24]. To measure the forces acting on the railhead, in contrast to the Schlumpf method [21], the signals are recorded from each strain gauge separately. In this case, to obtain the output signals, the strain gauges numbers 6 to 9 in **Figure 1** have been connected to four measuring bridges connected to the recording devices through strain amplifiers [22, 23]. Several calibration experiments were carried out to confirm the readings of strain gauges and force effects, including various options for loading the measuring section of the rail. As a result of calibration experiments using linear superposition from strain gauges ( $S$ ) readings, the influence matrix  $[G]$  has been formed. The pseudoinverse matrix  $[G]^+$  to the matrix  $[G]$  is calculated, which makes it possible to obtain at each moment ( $t$ ) the actual values of the force acting on rolling stock/rail interaction, according to the incoming signals from strain gauges using the matrix on Eq. (1) [22, 23]:

$$\{F(t)\} = \begin{Bmatrix} Q(t) \\ P(t) \\ M_z(t) \end{Bmatrix} = [G]^+ \cdot \{S(t)\}. \quad (1)$$

According to the calculations using the finite element method, it has been found that the restoration of lateral forces using the method of “Russian Railways-2016” [22, 27] gives an error of no more than 10%. In contrast, with the restoration of vertical forces, the relative error does not exceed 1.5%, and it has been noted that using the “RZD-2016” method compared with the Schlumpf method significantly increases the number of used strain gauges and measurement channels.

The researches of Yu.S. Romain [7] confirmed that to reduce the number of strain gauges and channels, measure the stresses not at four but three points of the rail, connecting them with three half-bridge circuits. As a result of theoretical and experiments calculations, the measurement error ratio was about 4% [7]. Later, numerous experimental studies in this field have been carried out, and the most important researches were proposed by D.R. Ahlbeck and H.D. Harrison [9, 28, 29] and by A. Moreau [30].

On the railways of North America and Europe, the “American Method” described by D.R. Ahlbeck and H.D. Harrison [9, 28, 29] is used to measure the wheel/rail interaction loads. According to this method, measurements of lateral forces are carried out by strain gauges located on the rail foot, as shown in **Figure 2**.

A linear dependence of the lateral forces measured by the “American method” on the displacement of the vertical force relative to the longitudinal plane of the rail has been revealed [31]. Moreover, this dependence gives an error in measuring the lateral force of no more than 4% [14]. Subsequently, experimental methods for measuring transverse forces based on measurements of deformations on the surface of the rail foot has been developed in [32, 33].

Also, there is another method for measuring lateral forces - the “method with measurements over the sleeper”, similar to the Schlumpf method [19, 20], where four strain gauges are installed vertically on the rail neck above the axis of the





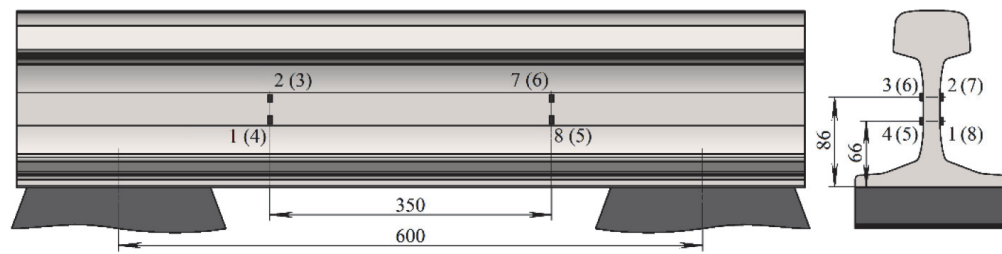


**Figure 3.**  
Location of strain gauges for determining lateral forces by the “French method”: 1–8 - numbers of strain gauges.

All the above methods for measuring the wheel/rail force are based on the use of strain gauges installed on the rail, differ in the location of strain gauges and the specifics of processing the received signals. Other experimental research methods of measuring the forces arising at the point of contact of wheel/rail are also known [14, 36, 38–41].

An effective method for measuring vertical and horizontal forces transmitted by wheels to sleepers are also methods where registration is carried out using force-measuring elements mounted on rail pads [3, 4, 40]. Such vertical and horizontal power measuring elements using strain gauges in the bridge circuit were developed at VNIIZhT by LA Grachishnikov [3].

In researches [38, 41], measurements of vertical and lateral forces from the wheel/rail interaction have been carried out by measuring the deformation of the hole in the rail. In this case, to measure the interaction forces, cylindrical strain gauges mounted on two liners have been installed in the holes in the rail neck [38] in the neutral axis of the rail, where each force component can be measured separately [14, 39]. Similarly, a simple transducer was developed that allows one to separate the effects of the vertical force from the lateral ones by placing it in the holes made in the rail neck near the centre of the rail lateral torsion [41]. The main disadvantages of the methods are the low sensitivity of deformation signals to lateral forces and violation of the track integrity [34, 35].

The statistical studies on the Russian railways showed that the GOST R 55050–2012 [21] method and the Russian Railways (RZD-2016) method are used to measure the force effect of rolling stock on the track [21, 27, 42]. These methods are implemented using strain gauges mounted on the rail neck and measure the wheel/rail forces only when the wheel is positioned over the strain gauges sections, and continuous registration of forces in the wheel /rail contact is impossible. In this case, the results depend on the speed of movement and the number of tests; therefore, to obtain a statistically reliable amount of experimental data, multiple passes of the test rolling stock along the measuring section of the track are required. For this reason, there is a need to develop new technical solutions that make it possible to increase the length of the measuring zone, ensure the continuous registration of the force effect wheel/rail interaction during movement, and increase the measurement accuracy.

## 2. Research on the development of methods for recording the wheel/rail interaction

### 2.1 Calculation method and calculation model

For this study, a simplified computational model of the rail track has been built, which is a rail of the R65 type (according to GOST 8161–75) [43], 3200 mm long, laid on six sleepers, the distance between them is 544 mm, with boundary

conditions characterizing the rigidity of the upper structure of the railway tracks, fasteners, and horizontal longitudinal stiffness of the rail, as shown in **Figure 4**.

As a boundary condition, kinematic connections have been assumed, which are elastic elements (Elastic Support/Foundation Stiffness), to consider the vertical and lateral stiffness of the relationship between the rail and sleepers and the longitudinal stiffness rail. In calculations, vertical and lateral forces added together in one section and successively have displaced along the rail. Different positions of the wheelset relative to the longitudinal axis of the rail during movement have been considered. **Figure 2** represents the Rail model that has been used where:

$Q$  - the vertical force;  $P$  - lateral force.

$l_1 = l_2 = l_3 = l_4 = l_5$  - the distance between the supports.

$a$  - represent the location of the vertical and lateral forces applied relative to the axis of symmetry of the inter-sleeper's gap.

$C_x$  and  $C_y$  - transverse (horizontal) and vertical stiffness of the connection between the rail and the sleepers.

$C_z$  - longitudinal stiffness of the rail.

Apply vertical loads on the rail's rolling surface; small areas of the contact patch with an area of  $144 \text{ mm}^2$  were provided (**Figure 3**). Contact patch centre:

- It is in the middle of the railhead.
- Displaced 11.7 mm outward from the middle of the railhead.
- Displaced 11.7 mm inward from the middle of the railhead.

Apply a lateral force to the rail's side edge; the ridge contact patch areas with an area of  $35 \text{ mm}^2$  were provided (**Figure 3**). The centre of such a platform was at a distance of 13 mm from the railhead level.

The ANSYS Workbench software package, version 18, has been used for calculations using the finite element method. The finite element mesh that has been

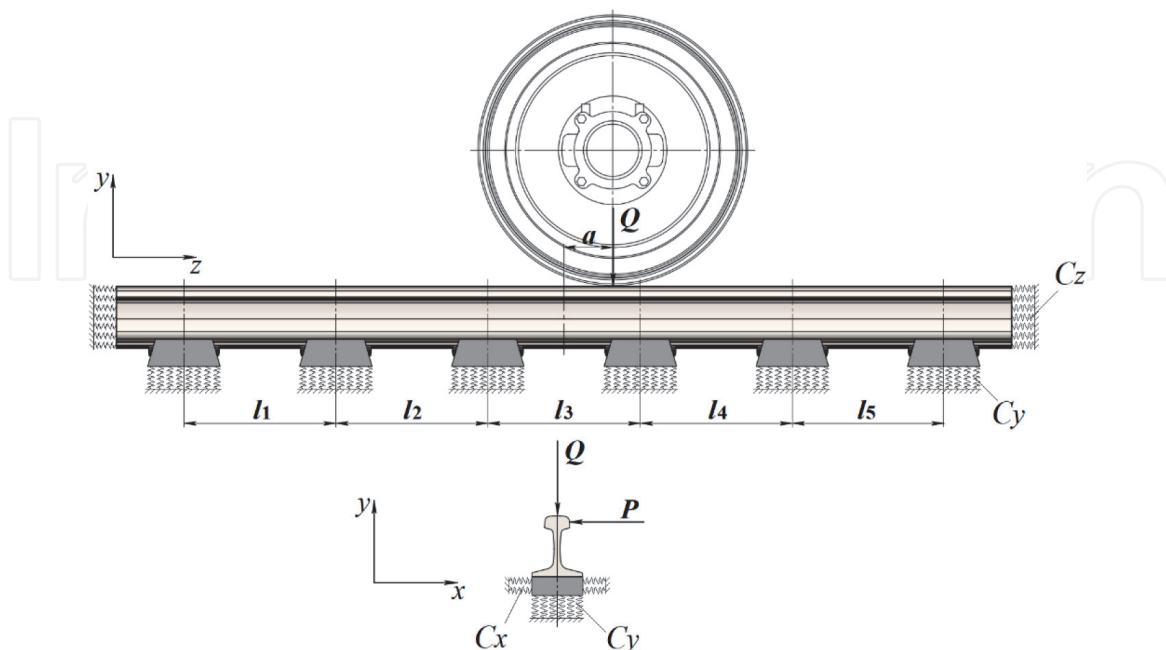


**Figure 4.** Design diagram of the rail, where:  $Q$  - the vertical force;  $P$  - lateral force;  $l_1 = l_2 = l_3 = l_4 = l_5$  - the length of the sleepers (distance between the supports);  $a$  - the coordinate of the application of vertical and lateral forces relative to the axis of symmetry of the inter-sleepers' gap;  $C_x$  and  $C_y$  - transverse (horizontal) and vertical stiffness of the connection between the rail and the sleepers;  $C_z$  - longitudinal stiffness of the rail.

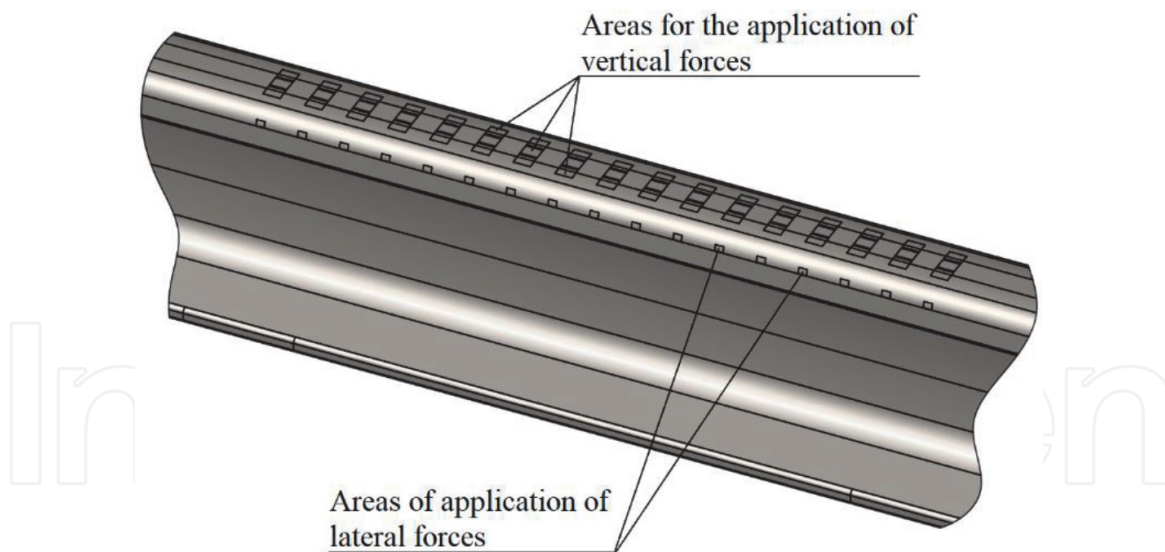


**Figure 5.**  
 Platforms on the rail surface for applying vertical and lateral forces.

applied to the rail model includes 117535 elements and 435738 nodes. Finite elements of the Solid186 type with a size of 7.5 mm have been used. The Solid186 feature has a quadratic shape with twenty nodes with three degrees of freedom at each node: displacements in the nodal coordinate system's x, y, and z directions.

The gap between the sleepers was divided into 17 sections to determine the dependence of the stresses arising on the surface of the rail neck, on the acting forces in the wheel/rail contact (from section -8 to section 8), the distance between which is 34 mm (**Figure 5**).

## 2.2 Research on the development of a method for registering vertical forces acting from a wheel on a rail

The analytical method of calculation substantiated the possibility of registering vertical forces from the wheel to the rail by measuring the shear stresses in two sections of the rail over a significant part of the sleep space [44, 45]. The results of the analytical calculation made it possible to conclude that the difference in shear forces in 2 symmetrical sections at a distance between the measuring sections remains constant and equal to the vertical force from the wheel to the rail (**Figure 6**).

$$P = Q1 - Q2 = \frac{I \cdot b}{S} (\tau_{zx}^L - \tau_{zx}^R) \quad (2)$$

Where,  $\tau_{zx}^L$  and  $\tau_{zx}^R$  - shear stresses, measured respectively in sections to the left and right of the acting force;  $S$  - the static moment of the lower part of the section relative to the point at which the stresses are determined;  $b$  - is the width of the rail neck in the measured section;  $I$  - the moment of inertia of the rail.

Since the calculation formulas (2) do not include parameters that depend on the distance between the sleepers and the characteristics of the supports, this circumstance makes it possible to determine the vertical force from the wheel to the rail on a significant part of the sleep distance, thereby increasing the volume of reliable statistical data obtained and increasing the accurate measurements.

Virtual measuring points were set symmetrically on both sides of the rail on the neutral axis, and the values from these points were summed up to check the



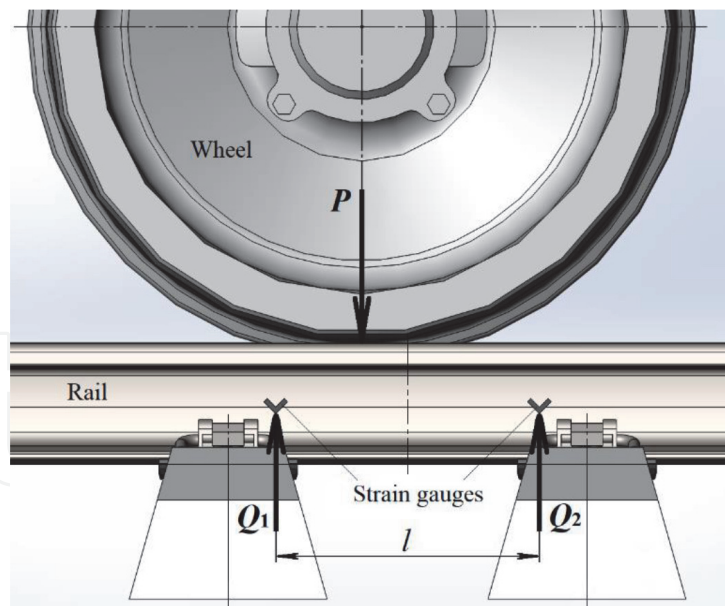


**Figure 6.** Scheme of piecewise continuous registration of vertical forces:  $P$  - vertical force from the wheel to the rail;  $Q_1$ ,  $Q_2$  - transverse forces;  $l$  - the distance between strain gauges.

possibility of restoring forces by measuring shear stresses in two sections and exclude the influence of lateral and longitudinal forces.

Using the FEM, the vertical force  $Q$  was applied at a point on the railhead surface for each section and alternately shifted along the rail from section  $-8$  to  $8$ . As a result, the reconstructed values of vertical forces were determined from the difference in shear stresses  $\tau_{zx(+i)} - \tau_{zx(-i)}$  arising in 2 symmetric sections of the rail when the vertical force moves along the rail, which are shown in **Figure 7**.

When comparing the calculation results of the vertical forces, it has been found that the main difference between the results obtained by the finite element method and the data found according to the beam theory was the absence of a force jump. Using FEM, a smooth increase in the values of the restored forces is observed over a length approximately equal to  $3/4$  of the rail height, then the growth slows down and reaches a maximum in the centre of the inter-sleeper gap. The forces at the centre of the span remain practically constant. The constant-scale zone for the restoration of the vertical force turns out to be significantly smaller than it follows from the calculation according to the beam theory.

The best accuracy of the vertical force is provided when measuring shear stresses in sections  $6$  ( $-6$ ) with a length of the measuring zone of about  $200$  mm (**Figure 7, d**). With an increase in the length of the measuring zone, the deviation increases. The accuracy of restoring the vertical force along sections  $4$  ( $-4$ ) and  $5$  ( $-5$ ) is significantly lower (**Figure 7, b, c**), but in the middle part of the measuring zone of any of these figures, the constancy of the restoring force is ensured. The resulting discrepancies can be eliminated by calibration. The maximum length of the measuring zone, where the constancy of the vertical force is ensured, is approximately  $0.3 \dots 0.5$  of the distance between the sections, which makes it possible to increase the volume of reliable statistical data obtained and improve the measurement accuracy.

Thus, the results obtained in the calculations by the finite element method confirmed the sufficient efficiency of restoring the vertical force in the wheel/rail contact from the measured shear stresses in two sections of the rail.

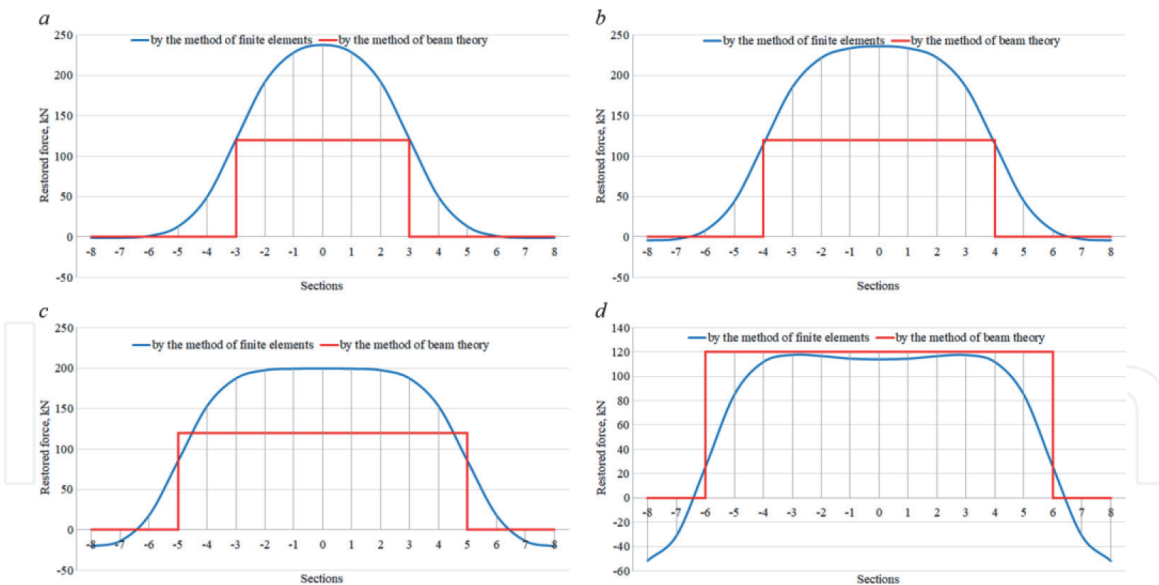


**Figure 7.**  
 The reconstructed values of the vertical force from the difference in the values of the shear stresses arising in the investigated sections of the rail when the vertical force moves from section  $-8$  to section  $8$ : a - section  $3$  ( $-3$ ); b - sections  $4$  ( $-4$ ); c - sections  $5$  ( $-5$ ); d - sections  $6$  ( $-6$ ).

### 2.3 Influence evaluation on the accuracy of displacement measurements of the wheel from the axis of symmetry and the occurrence of lateral forces

When the rolling stock moves along the rail track, a transverse displacement of the wheel pair in the track occurs, which leads to the displacement of the “wheel/rail” contact patch in the transverse plane of the rail; as a result, the vertical force also changes its position. In this case, the occurrence of lateral force is possible when the wheel flange hits the rail. Therefore, additional calculations were carried out for the following cases: displacement of the point of application of the vertical force relative to the longitudinal axis of the rail; lateral force generation.

As a result of the calculations, taking into account the movement of the wheel/rail contact patch in the transverse plane and the occurrence of lateral force, it was found that the lateral displacement of the wheel relative to the longitudinal plane of the rail by  $11.7$  mm and the occurrence of lateral force do not significantly affect the measurement accuracy of the vertical forces by the difference between the values of shear stresses in two sections of the rail. In this case, the effect of the lateral displacement of the wheelset on the result is no more than  $1.6\%$ , and the lateral force is no more than  $1.38\%$ .

For further experimental verification, it has been recommended to install strain gauges in sections  $6$  ( $-6$ ), provided that the distance between the axles of the sleepers is  $544$  mm and the length of the sleeper gap is  $408$  mm. The stiffness characteristics of the rail base and rail can influence the results of the experiment. The discrepancy between the vertical force coming from the wheel to the rail and the restoring force is proposed to be eliminated by calibrating the strain gauge circuits.

### 2.4 Experimental studies to determine the loads from a wheel/rail contact

Experiments were carried out on a fragment of an R65 type rail made according to GOST 8161–75 [43] with a length of  $665$  mm, fixed on two supports measuring  $200 \times 140 \times 20$  mm; distance is  $544$  mm.

Pre the experiment, a precision marking of a rail fragment between the supports was carried out on 17 sections, the distance between 34 mm.

Then, strain gauges were glued to both sides of the rail web. Strain gauges are placed on the neutral axis of the rail in sections 6 (–6) to determine the vertical force by measuring the stresses in two sections of the rail. To determine the forces on the rail, strain gauges have been installed on the neutral axis of the rail in section 0. The arrangement of strain gauges is shown in **Figure 8**.

Strain gauges are connected to two full parallel bridges with a four-wire connection to register signals in sections –6 (6). Strain gauges are connected according to a full-bridge circuit with a four-wire connection to register signals in section 0.

$$P = Q_1 - Q_2 = \frac{K_p(\varepsilon_1 + \varepsilon_2)}{2} - \frac{K_p(\varepsilon_3 + \varepsilon_4)}{2} - \frac{K_p(\varepsilon_5 + \varepsilon_6)}{2} + \frac{K_p(\varepsilon_7 + \varepsilon_8)}{2} = \frac{K_p}{2}(\varepsilon_1 + \varepsilon_2 - \varepsilon_3 - \varepsilon_4 - \varepsilon_5 - \varepsilon_6 + \varepsilon_7 + \varepsilon_8), \quad (3)$$

Where  $Q_1 - Q_2$  is the difference in shear forces.

$K_p$  is a coefficient that depends on the characteristics of the material and the profile of the rail. During operation, this factor can change due to wear on the railhead.

The change in the output voltage for the considered circuit of parallel operation of two bridges is determined by the expression:

$$\Delta U = k(\varepsilon_1 + \varepsilon_2 - \varepsilon_3 - \varepsilon_4 - \varepsilon_5 - \varepsilon_6 + \varepsilon_7 + \varepsilon_8)(1 - \eta)U, \quad (4)$$

or

$$\Delta U = k \cdot \varepsilon_\Sigma(1 - \eta)U. \quad (5)$$

$$\varepsilon_\Sigma = \varepsilon_1 + \varepsilon_2 - \varepsilon_3 - \varepsilon_4 - \varepsilon_5 - \varepsilon_6 + \varepsilon_7 + \varepsilon_8;$$

Where  $\eta$  is a term characterizing the nonlinearity of the bridge;  $k$  - coefficient of sensitivity of strain gauges;  $U$  is the voltage of the measuring bridge.

From equality (3) and (5), we obtain the formula for determining the vertical force from the readings of strain gauge bridges:

$$P = \frac{K_p}{2} \varepsilon_\Sigma = \frac{K_p}{2} \frac{\Delta U}{Uk(1 - \eta)}. \quad (6)$$

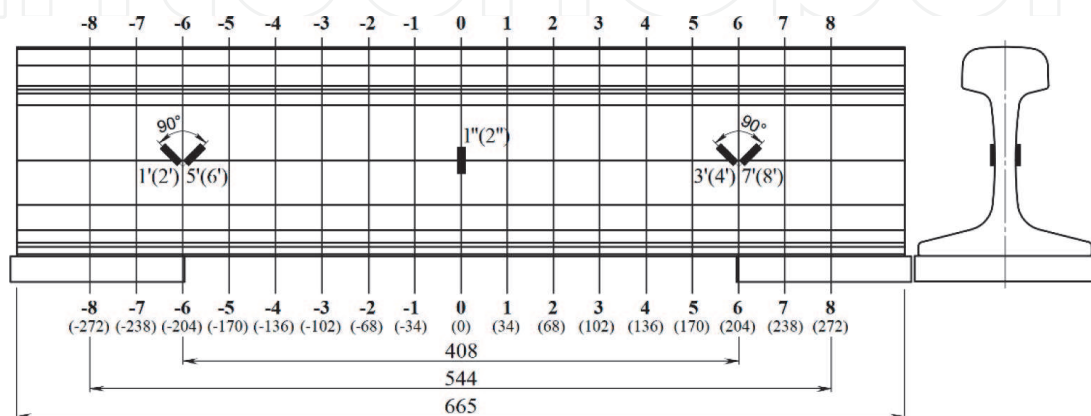


**Figure 8.**

Layout of strain gauges on the rail neck (numbers from –8 to 8 indicate section numbers, numbers in brackets for each section indicate distances from the middle part between the supports): 1'–8', 1''–2'' - strain gauge numbers.

During experiments, a static vertical load  $P$  equal to 0 kN, then from 100 kN to 200 kN with a step of 25 kN was applied to a rail fragment sequentially, along the investigated sections (Figure 8), through a loader at the DYNASET-200 stand. Up to 100 kN to 0 kN with the same step until the moment of complete unloading. The experiment process at the DYNASET-200 stand is shown in Figure 9.

Based on experiments results, the dependences of the vertical force on the position of the load application point have been determined according to the proposed method (Figure 10).

The experiment results showed that the average value of the restored forces over the length of the measuring zone of 204 mm according to measurements in sections 6 (–6) was  $199.15 \pm 0.98$  kN with a load of 200 kN. The error ratio, in this case, was equal to 0.42%.

The experiments were carried out to determine the vertical static force from the wheel to the rail according to the proposed method based on the measured stresses in two rail sections.

The results showed that the discrepancies in the recovery of the force value of 200 kN at the point of application of the vertical force located in the longitudinal axis of the rail, in section 0 according to measurements in sections 6 (–6) relative to the measuring circuit located in section 0 and recording readings according to GOST R 55050–2012 [21], was 0.47% (0.95 kN).

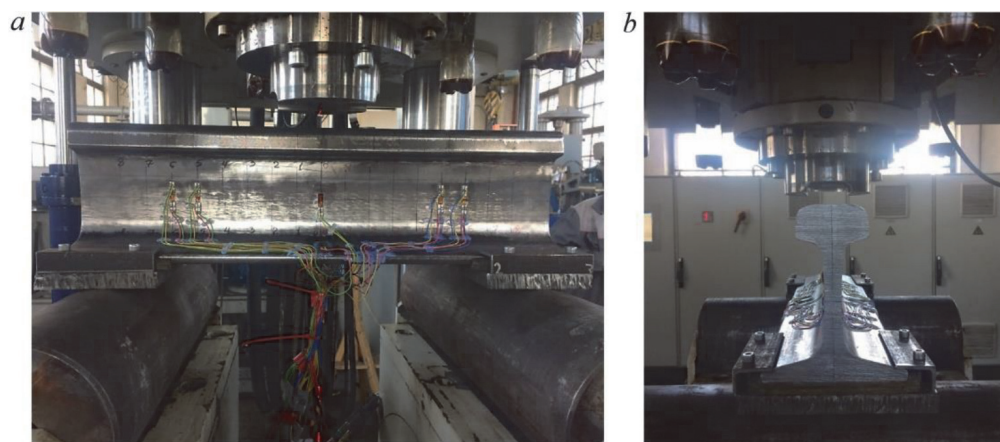


**Figure 9.**  
 A fragment of a rail on the DYNASET-200 stand during the experiment: a) front view: b) left view.

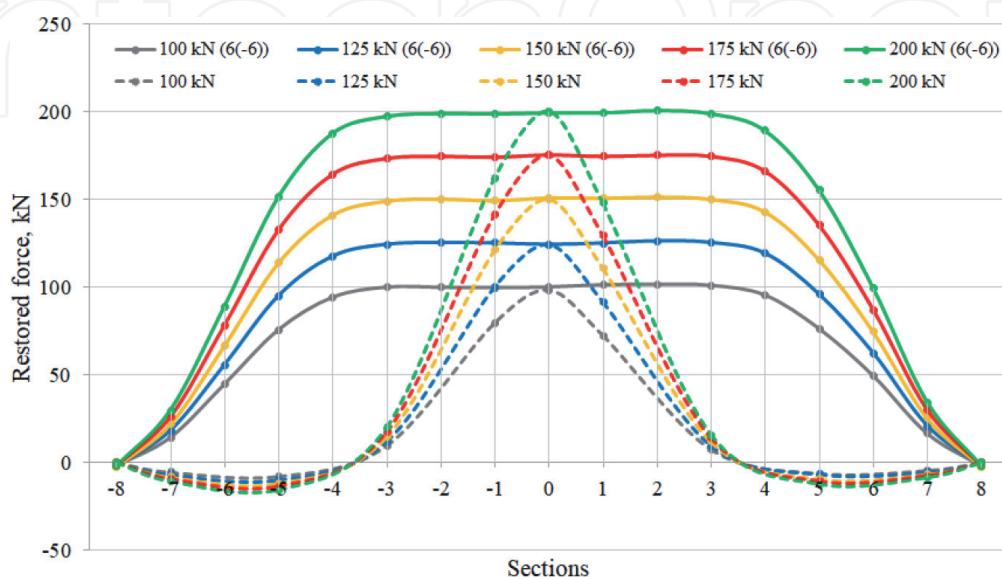


**Figure 10.**  
 Dependence of the restored forces recorded by the measuring circuits located in sections 6 (–6).



Thus, the experimental studies confirmed the effectiveness of recovering vertical forces by measuring stresses in two sections of the rail under the action of a vertical load located in the longitudinal plane of the rail [46, 47].

Then, the proposed measurement technology has been tested to determine the wheel/rail interaction loads [48, 49]. Due to the nature of the track on the site, strain gauges have been installed at 363 mm.

Over a length of the measuring zone of approximately 220 mm, the deviations of the scale factor from the mean value do not exceed 3%, which is in satisfactory agreement with the FEM calculation. It is also possible to increase the length of the measuring zone up to  $\pm 440$  mm when using a variable scale factor. The measurement comparison results are shown in **Figure 11**.

It is clear that, at the moment when the wheel was passing the middle of the measuring section, the results coincide with the measurements according to GOST R 55050–2012, and the proposed method gives many values of the rolling stock/rail interaction force.

Thus, the results above confirmed the ability of the new method to determine the vertical force acting in the wheel/rail interaction, increase the information received by 20–40 times with the same number of measuring circuits and improve the measurement accuracy compared with the current method using according to GOST R 55050–2012 [50].

## 2.5 Development of a method for determining lateral forces in the wheel/rail interaction

To develop a new method for measuring the lateral force from the wheel/rail interaction theoretically, the method of registering vertical forces between the wheel/rail by measuring stresses in two sections of the rail [44, 50] and the “French method” of lateral forces registration has been adopted as prototypes, The method of registering vertical forces between the wheel/rail by measuring stresses in two sections of the rail increased measurement accuracy of the vertical effect of the rolling stock on the path on a significant part of the sleeper gap. The “French

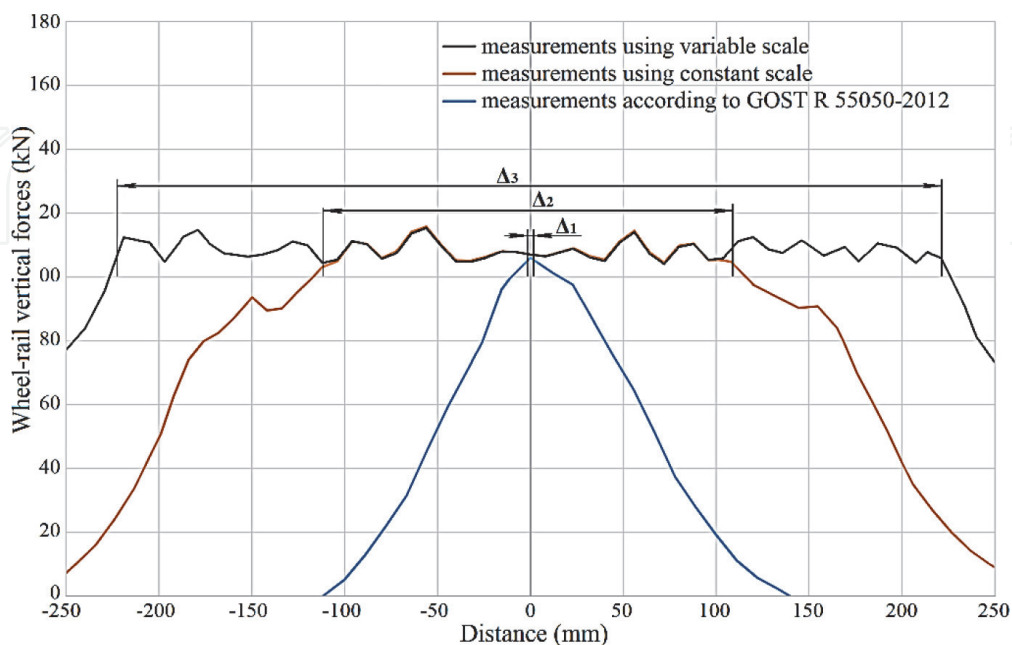


**Figure 11.**

The measurement of the vertical force acting from the wheel to the rail when passing the measuring section at a speed of 100 km / h (length of the measuring zone with an error of no more than 3%  $\Delta_1 \approx 8$  mm), according to the method of two sections with a constant scale ( $\Delta_2 \approx 220$  mm) and variable scale ( $\Delta_3 \approx 440$  mm).



method” of lateral forces registration, described in [31, 30], with the installation of strain gauges vertically on the rail necks, symmetrically relative to the horizontal neutral axis of the rail.

At the first stage, the results accuracy of the “French method” was investigated on the track of a traditional 1520 mm gauge design [30]. For this, eight virtual measuring points have been installed on both sides of the rail neck in two vertical cross-sections located in the inter-sleep space.  $Ly_1 - Ly_2$  values were changed while maintaining the symmetrical arrangement of the measurement points relative to the neutral axis of the rail (**Figures 12**). The  $(Ly_1 - Ly_2)$  in the vertical direction between the measurement points varied from 5 to 90 mm with a step of 5 mm. The distance in the horizontal direction was varied from 274 to 544 mm with a step of 10 mm.

In this case, the lateral force  $P$  is determined, similarly to the Schlumpf method [19], by the expression.

$$P = \frac{M_{O_1} - M_{O_2}}{L_{y2} - L_{y1}} = \frac{\Delta M}{\Delta L_y}, \quad (7)$$

Here  $M_{O_1}, M_{O_2}$  are the bending moments relative to the points  $O_1$  and  $O_2$  (**Figure 12**) from the action of the vertical force  $Q$  and lateral force  $P$ .

As a result of multivariate calculations using the finite element method, the dependences of the main, normal, and tangential stresses arising in the investigated sections of the rail under the action of vertical and lateral forces have been obtained.

The calculations showed that with such an arrangement of measuring points, it is impossible to accurately determine the value of the lateral force (railway track with R65 rails and laying concrete sleepers 1800 pcs / km) [51].

The maximum error ratio of expression (7) was no more than 13.8%, caused by the nonlinear dependence of the stresses  $\sigma_y$  on the displacement of the contact point in the transverse direction. Therefore, it has been decided to abandon the “French” approach to measurements with the asymmetrical installation of measurement points relative to the neutral axis of the rail.

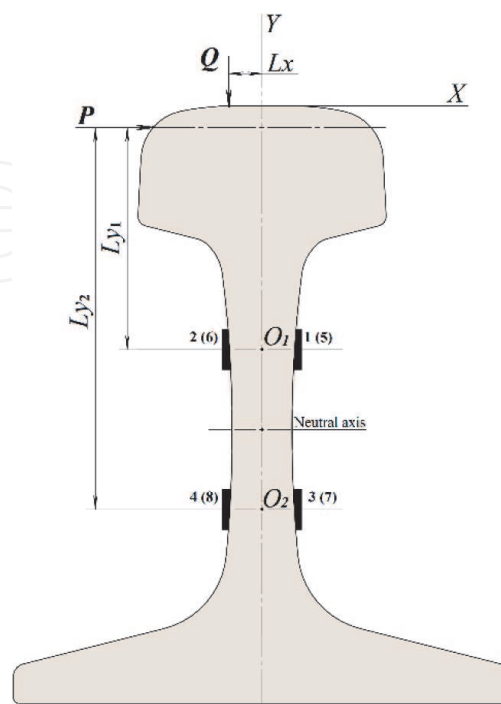


**Figure 12.**

Arrangement of symmetrical points for measuring voltages; 1–8 - numbers of points of measurements;  $Q$  is the vertical force;  $P$  - lateral force;  $X, Y$  - directions of the axes of the coordinate system.

At the second stage, multivariate calculations have been carried out to measure normal stresses at the points without maintaining the symmetrical arrangement of the measurement points relative to the neutral axis of the rail. The best results determine lateral forces from the wheel/rail interaction given by the location of the measurement points below the neutral axis of the rail (**Figure 13**).

At the designated points, the values of normal stresses  $\sigma_y$  are determined. The differences in normal stresses ( $\sigma_y$ ) do not depend on the displacement of the vertical force across the rail, and expression (7) has been used to determine the lateral force, as in the Schlumpf method. The value of  $\Delta L_y$  is constant. The arising stresses linearly depend on  $\Delta M$ ; therefore, expression (7) has been replaced with the equivalent:

$$P = \frac{\Delta M}{\Delta L_y} = K \Delta \sigma_y. \quad (8)$$

Where  $K$  is a scale factor that depends on the inertial characteristics of the rail section;  $\Delta \sigma_y$  is the difference between normal stresses arising at points (**Figure 13**), which is determined by the formula:

$$\Delta \sigma_y = (\Delta \sigma_{y34} + \Delta \sigma_{y78}) - (\Delta \sigma_{y12} + \Delta \sigma_{y56}) \quad (9)$$

where  $\Delta \sigma_{y12}$ ,  $\Delta \sigma_{y34}$ ,  $\Delta \sigma_{y56}$  and  $\Delta \sigma_{y78}$  are the values of the difference between the normal stresses at the measuring points 1 2; 3 4; 5 6 and 7 8, respectively, determined by the formulas:

$$\Delta \sigma_{y12} = \sigma_{y1} - \sigma_{y2}; \Delta \sigma_{y34} = \sigma_{y3} - \sigma_{y4}; \Delta \sigma_{y56} = \sigma_{y5} - \sigma_{y6}; \Delta \sigma_{y78} = \sigma_{y7} - \sigma_{y8}. \quad (10)$$

The values of  $\Delta \sigma_y$  has been determined according to formula (9) in the central part of the sleeper do not depend on vertical force application relative to the middle of the railhead. However, they have some deviations along the measuring zone, from section  $-8$  to section  $8$ ; with an increase in length, the deviation increases.

Thus, the values of  $\Delta \sigma_y$  was obtained when multiplied by a scale factor, make it possible to determine the magnitude of the lateral force during the wheel/rail interaction.

The analysis of the results using FEM confirms that such an arrangement of measurement points using a constant scale factor provides a standard deviation

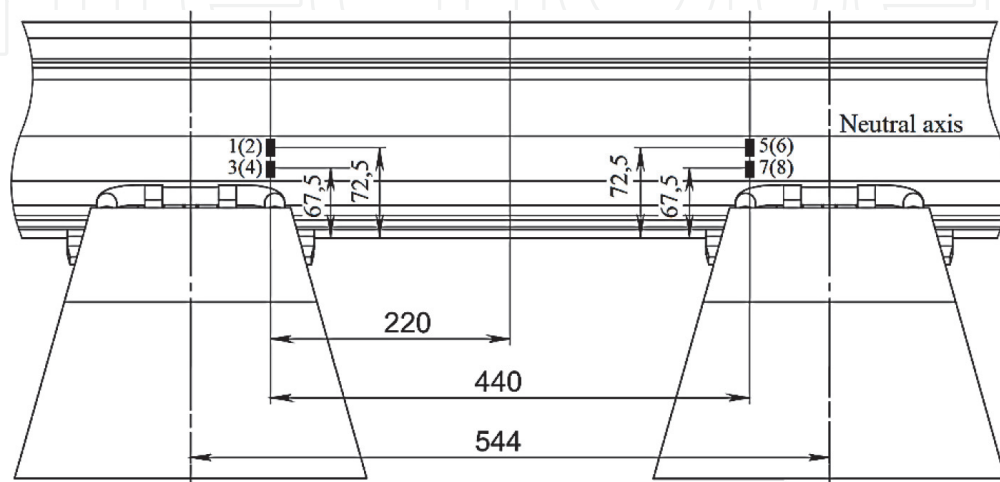


**Figure 13.**

Layout of stress measurement points below the neutral axis of the rail: a - view from the inside of the track; b - outside view; 1-8 sampling point numbers.

when determining the wheel/rail interaction lateral force of no more than 4% along the length of the measurement zone of approximately 140 mm. The values of the wheel/rail interaction lateral force when a vertical force of 120 kN and a lateral force of 45 kN have been applied are shown in **Figure 14**.

From the above results, lateral forces of the wheel/rail interaction along the length of the 140 mm measuring zone with a relative error of not more than 4.0% have been determined by installing eight strain gauges in the inter-sleeper span below the neutral axis of the rail and perpendicular to the longitudinal axis of the rail. Strain gauges are installed on both sides of the rail web in two vertical cross-sections, the distance between which is 440 mm, provided that the distance between the sleepers' axes is 544 mm to eliminate the influence on the measurement accuracy of lateral forces from the wheel/rail interaction and the displacement of vertical forces relative to the longitudinal plane of the rail. The sections are located symmetrically at a distance of 220 mm from the vertical central transverse plane of the sleepers. Strain gauges with a 1–5 mm base are glued at heights of 67.5 and 72.5 mm from the rail base. The developed method for measuring lateral forces by measuring normal stresses in two rail sections is recommended to be verified experimentally.

## 2.6 Experimental studies to determine lateral loads from the interaction of a wheel with a rail

Experiments have been carried out on a fragment of a railway track with R65 rails according to GOST 8161–75 [43], 3000 mm long, laid on wooden supports (beams) measuring 100 × 200 × 2000 mm, the spacing of which is 544 mm. A precision marking of the R65-type rail was carried out between wooden beams in 9 sections, the distance between which is 34 mm to prepare for the experimental tests. Precision rail markings are shown in **Figure 15**.

Then, on both sides of the rail web in two vertical cross-sections with the distance between them 440 mm, strain gauges with a nominal base of 3 mm have been glued. The sections have been arranged symmetrically at a distance of 220 mm from the vertical central transverse plane between the wooden beams. At the same

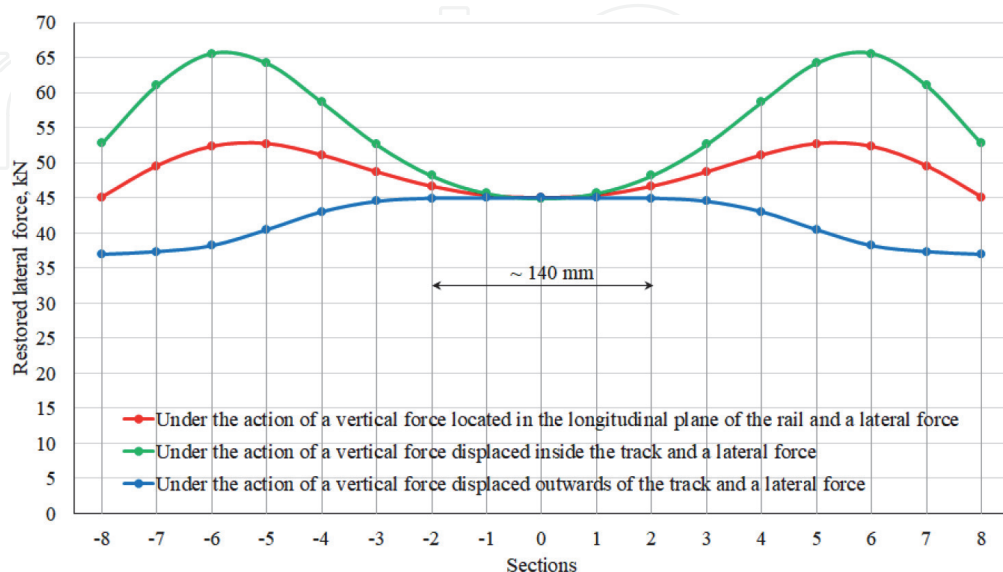


**Figure 14.**

The values of the lateral force from the difference in the values of the normal stresses arising in the investigated sections of the rail when the vertical and lateral forces move from section - 8 to section 8. (The lateral force in the rail calculate according to Eq. 5, and when vertical force 120kN and lateral force of 45 kN acted on the rail).

time, in contrast to theoretical studies [51], where the distance between the measurement points is recommended to be 5 mm, in experimental studies, the distance between the centres of the strain gauges was 7 mm. When the wheel moves along the rail and sleepers, deformations occur, recorded by the installed strain gauges. The vertical normal stress  $\sigma_{yi}$  arising on the rail web is proportional to the deformations.

$$\sigma_{yi} = \frac{E}{1 - \mu^2} (\varepsilon_{yi} + \mu\varepsilon_{xi}), \quad (11)$$

Where  $E$  is the modulus of elasticity;  $\mu$  is Poisson's ratio;  $\varepsilon_{yi}$  - linear deformations caused by normal stresses  $\sigma_{yi}$  on the rail web;  $\varepsilon_{xi}$  - linear deformations on the rail web caused by rail bending.

The difference between normal stresses, expressed in terms of deformations, has the following form:

$$\Delta\sigma_{y12} = \sigma_{y1} - \sigma_{y2} = \frac{E}{1 - \mu^2} (\varepsilon_{y1} - \varepsilon_{y2}); \quad (12)$$

$$\Delta\sigma_{y34} = \sigma_{y3} - \sigma_{y4} = \frac{E}{1 - \mu^2} (\varepsilon_{y3} - \varepsilon_{y4}); \quad (13)$$

$$\Delta\sigma_{y56} = \sigma_{y5} - \sigma_{y6} = \frac{E}{1 - \mu^2} (\varepsilon_{y5} - \varepsilon_{y6}); \quad (14)$$

$$\Delta\sigma_{y78} = \sigma_{y7} - \sigma_{y8} = \frac{E}{1 - \mu^2} (\varepsilon_{y7} - \varepsilon_{y8}); \quad (15)$$

$$\begin{aligned} \Delta\sigma_y &= (\Delta\sigma_{y34} + \Delta\sigma_{y78}) - (\Delta\sigma_{y12} + \Delta\sigma_{y56}) \\ &= \frac{E}{1 - \mu^2} (\varepsilon_{y3} - \varepsilon_{y4} + \varepsilon_{y7} - \varepsilon_{y8} - \varepsilon_{y1} + \varepsilon_{y2} - \varepsilon_{y5} + \varepsilon_{y6}). \end{aligned} \quad (16)$$

Where  $\varepsilon_{yi}$  is deformations caused by normal stresses  $\sigma_{yi}$  recorded by the  $i$ -th strain gauge.

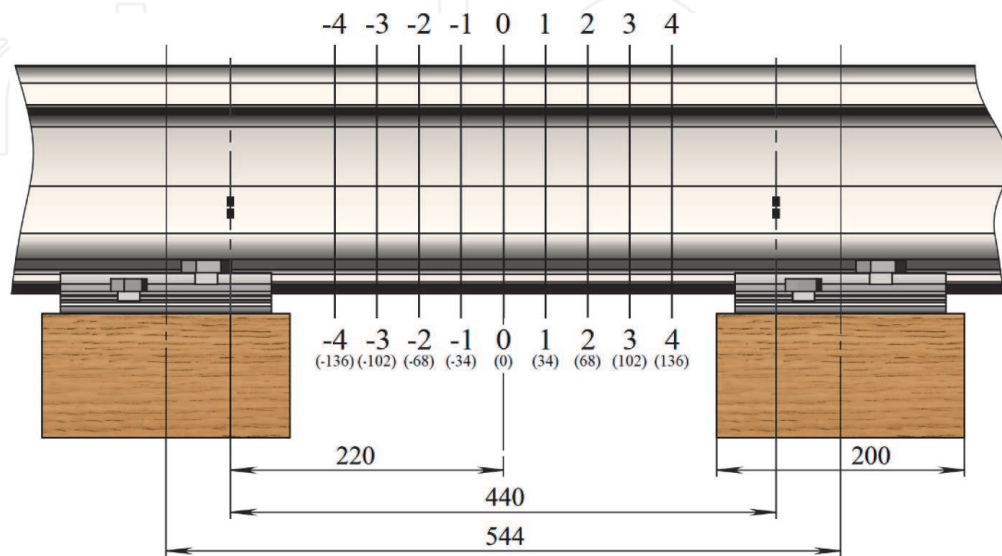


**Figure 15.** Sections of the investigated rail fragment between the sleepers (numbers from  $-4$  to  $4$  indicate the section numbers, the numbers in brackets for each section indicate the distance from the middle part between the wooden beams).

The magnitude of the lateral force, expressed in terms of deformations  $\varepsilon_{yi}$ , has the form:

$$P = K \cdot \Delta\sigma_y = K \cdot \frac{E}{1 - \mu^2} (\varepsilon_{y3} - \varepsilon_{y4} + \varepsilon_{y7} - \varepsilon_{y8} - \varepsilon_{y1} + \varepsilon_{y2} - \varepsilon_{y5} + \varepsilon_{y6}) \quad (17)$$

The summation and subtraction of strain signals included in the formula (17) are performed using a complete measuring bridge with a four-wire connection. The expression determines the change in the output voltage of the measuring bridge:

$$\Delta U = \left( \frac{\Delta R_3}{R} - \frac{\Delta R_4}{R} + \frac{\Delta R_7}{R} - \frac{\Delta R_8}{R} - \frac{\Delta R_1}{R} + \frac{\Delta R_2}{R} - \frac{\Delta R_5}{R} + \frac{\Delta R_6}{R} \right) (1 - \eta) U, \quad (18)$$

$R$  is the resistance of the strain gauges;  $\Delta R_1 - \Delta R_8$  - change in resistance of strain gauges T1 – T8, respectively;  $\eta$  - parameter characterizing the nonlinearity of the measuring bridge;  $U$  is the voltage of the measuring bridge.

The resistance change is proportional to the deformation.

$$\frac{\Delta R_i}{R} = k_T \varepsilon_{yi}, \quad (19)$$

Where  $k_T$  is the coefficient of the strain gauge sensitivity of the strain gauges. Then the change in the output voltage will be determined by the formula:

$$\Delta U = k_T (\varepsilon_{y3} - \varepsilon_{y4} + \varepsilon_{y7} - \varepsilon_{y8} - \varepsilon_{y1} + \varepsilon_{y2} - \varepsilon_{y5} + \varepsilon_{y6}) (1 - \eta) U \quad (20)$$

From expressions (17) and (20), we obtain the formula for calculating the lateral forces arising from the interaction of the wheel and the rail:

$$\begin{aligned} P &= K \frac{E}{1 - \mu^2} (\varepsilon_{y3} - \varepsilon_{y4} + \varepsilon_{y7} - \varepsilon_{y8} - \varepsilon_{y1} + \varepsilon_{y2} - \varepsilon_{y5} + \varepsilon_{y6}) = \\ &= K \cdot \frac{E}{1 - \mu^2} \cdot \frac{\Delta U}{k_T U (1 - \eta)} = K_{sp} \cdot \frac{\Delta U}{U (1 - \eta)}, \end{aligned} \quad (21)$$

Where  $K_{sp} = K \frac{E}{k_m (1 - \mu^2)}$  - it is proposed to determine experimentally.

To register signals and determine lateral forces during the wheel/rail according to expression (21) is necessary to install eight strain gauges vertically on both sides of the rail neck, connected to a complete measuring bridge with a four-wire circuit with recording equipment.

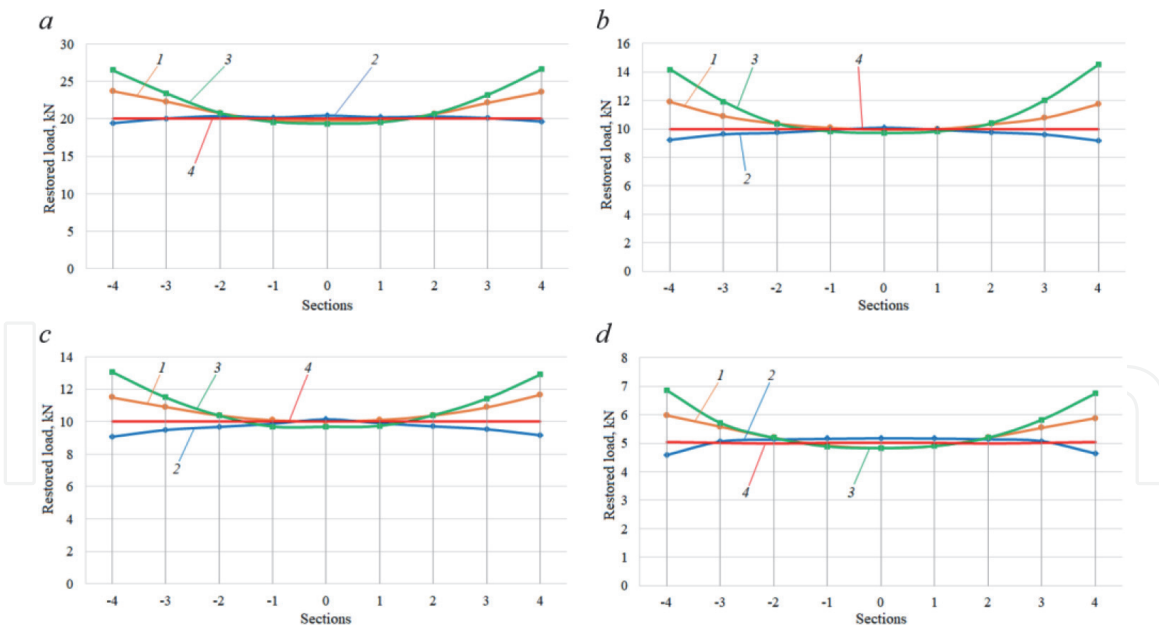
At the first stage, a central vertical static load  $Q$ , equal to 25 and 50 kN, have been applied sequentially (**Figure 15**), followed by a decrease in the load until the moment of complete unloading.

At the second stage of the experiment, a vertical static load  $Q$ , equal to 25 and 50 kN, was applied along the rail sections with a displacement relative to the longitudinal rail axis by 20 mm outward and inward from the middle of the railhead. At all stages of the experiment, simultaneously with the vertical load on rail fragment, a horizontal transverse load  $P$  equal to  $0.2Q$  and  $0.4Q$  have been applied at a distance of 20 mm from the railhead level.

According to the experiment results [52], the dependences of the lateral force on the point of load application have been determined using the proposed method (**Figure 16**).

The average values of the restored lateral forces over the length of the measuring zone 136 mm have been obtained, shown in **Table 1**.




**Figure 16.**

Dependences of the restored lateral forces on the point of load application: a - under the action of a vertical force of 50 kN and a lateral force of 20 kN; b - under the action of a vertical force of 50 kN and a lateral force of 10 kN; c - under the action of a vertical force of 25 kN and a lateral force of 10 kN; d - under the action of a vertical force of 25 kN and a lateral force of 5 kN; 1 - under the action of a vertical force in the longitudinal plane of the rail and a lateral force; 2 - under the action of a vertical force with an outward displacement of the track and lateral force; 3 - under the action of a vertical force with an inward displacement of the track and lateral force; 4 - actual load.

Parameter	Loading Scheme			
	A	B	C	D
Recovered loads, kN:				
mean	20.16	10.04	10.02	5.06
maximum value	20.79	10.38	10.39	5.20
minimum value	19.35	9.71	9.68	4.84
Confidence interval width, kN	0.72	0.34	0.36	0.18
Standard deviation, kN	0.47	0.24	0.28	0.15
Relative error, %	2.37	2.43	2.82	3.01

A - with a vertical force of 50 kN and a lateral force of 20 kN;  
 B - with a vertical force of 50 kN and a lateral force of 10 kN;  
 C - With a vertical force of 25 kN and a lateral force of 10 kN;  
 D - With a vertical force of 25 kN and a lateral force of 5 kN.

**Table 1.**

Statistical data obtained from the length of the measuring section (136 mm).

The experimental studies carried out on the railway track confirmed the results of theoretical studies and the effectiveness of the method of piecewise continuous recording of lateral loads from the wheel/rail interaction by measuring the normal stresses in two rail sections [53].

### 3. Conclusions and recommendations

1. Theoretically and experimentally approved the possibility of piecewise continuous recording of vertical and lateral forces from the wheel/rail

interaction by measuring the stresses in two rail sections on a significant part of the sleeper gap.

2. As a result of comprehensive studies using analytical calculations on beam theory, the finite element method and experiments on stands and railway tracks, it has been approved that the best option for determining the vertical forces in wheel/rail contact by measuring shear stresses in two sections of the rail when installing strain gauges on the neutral axis of the rail in two sections at a distance of 204 mm from the centre of the sleeper gap (the distance between the measuring sections is 408 mm). This ensures the determination of the vertical force with a relative error of not more than 4% over the length of the measuring zone, approximately 1/3 of the distance between the sleepers (approximately 220 mm), and with the use of a variable scale factor, this length increases to 440 mm.
3. As a result of comprehensive studies using the finite element method and experiments on the railway track, it has been found that the best option for determining lateral forces from the wheel/rail interaction by measuring normal stresses in two sections of the rail and install eight strain gauges at heights of 67.5 and 72.5 mm from the rail base in two vertical cross-sections, the distance between them is 440 mm, located symmetrically relative to the vertical central transverse plane of the sleepers gap. This arrangement of strain gauges provides a standard deviation of the restored lateral force of no more than 4% along the length of the measuring zone of about 140 mm.
4. Thus, methods and devices have been developed for determining the vertical and lateral forces acting from the wheel on the rail by measuring the stresses in two sections of the rail [54, 55], which ensure the registration of the force effect of the rolling stock on the railway track on a significant part of the sleeper gap, allowing to increase the volume the obtained reliable statistical data, improve the measurement accuracy, reduce the number of trips of the tested rolling stock along the experimental measuring sections, thereby reducing the time and cost of tests in comparison with test according to GOST R 55050-2012 and “RZD-2016”.
5. The developed methods for measuring the forces of wheel/rail interaction by measuring stresses in two sections of a rail has been recommended to be used when determining the wheel/rail interaction forces, as well as for identifying defects on the rolling surface of wheels when diagnosing rolling stock while a train is in motion [56, 57].

IntechOpen

### **Author details**

Yuri P. Boronenko<sup>1</sup>, Rustam V. Rahimov<sup>2</sup> and Waail M. Lafta<sup>3\*</sup>

1 St. Petersburg State Transport University, St. Petersburg, Russia

2 Tashkent State Transport University, Tashkent, Uzbekistan

3 Martinus Rail Pty Ltd., Brisbane, Australia

\*Address all correspondence to: waelwe@yahoo.com

### **IntechOpen**

---

© 2021 The Author(s). Licensee IntechOpen. This chapter is distributed under the terms of the Creative Commons Attribution License (<http://creativecommons.org/licenses/by/3.0>), which permits unrestricted use, distribution, and reproduction in any medium, provided the original work is properly cited. 

## References

- [1] Ershkov O.P., Calculation of lateral horizontal forces in curves. Proceedings of the Central Research Institute of the Russian Ministry of Railways. Issue 301. Moscow: Transport, 1966. 235 p.
- [2] Kogan A. Ya., Nikitin D.A., Poleshchuk I.V., Oscillations of the track at high vehicle speeds and impact interaction of the wheel and rail. Moscow: Intekst, 2007. 168 p.
- [3] Verigo M.F., Kogan A. Ya. Interaction between track and rolling stock. Moscow: Transport, 1986. 559 p.
- [4] Bromberg E.M., Verigo M.F., Danilov V.N., Frishman M.A. Interaction between track and rolling stock. Moscow: Transzheldorizdat, 1956. 280 p.
- [5] Frishman M.A. Studies of the interaction of the track and rolling stock by filming. Moscow: Transzheldorizdat, 1953. 116 p.
- [6] Eliseev K.V. Modern methods for determining the forces in contact between a wheelset and rails. Modern mechanical engineering. Science and education. 2014. No. 4. P. 867–876.
- [7] Romen Yu. S., Suslov O.A., Balyaeva A.A. Determination of the interaction forces in the wheel-rail system based on the measurement of stresses in the rail web. VNIIZhT Bulletin. 2017. Vol. 76. No. 6. P. 354–361.
- [8] Danilov V.N. Railway track and its interaction with rolling stock. Moscow: Transzheldorizdat, 1961. 112 p.
- [9] Ahlbeck D.R., Harrison H.D. Techniques for measurement of wheel-rail forces. The Shock and Vibration Digest. 1980. Vol. 12. No. 10. P. 31–41.
- [10] Vershinsky S.V., Danilov V.N., Khusidov V.D. The dynamics of the car: a textbook for higher educational institutions of the railway. Transport. Moscow: Transport, 1991. 360 p.
- [11] Ershkov O.P. Establishing coefficients that take into account the lateral bending and torsion of the rails. Proceedings of the Central Research Institute of the Ministry of Railways. Issue 97. Moscow: Transzheldorizdat, 1955. S. 289–325.
- [12] Shafranovsky A.K. Measurement and continuous registration of forces of interaction of wheel pairs of locomotives with rails. VNIIZhT Proceedings. Issue 389. Moscow: Transport, 1969. 119 p.
- [13] Shafranovsky A.K. Continuous registration of vertical and lateral forces of interaction between the wheel and the rail. VNIIZhT Proceedings. Issue 308. Moscow: Transport, 1965. 96 p.
- [14] Brzhezovsky A.M. Methods for Experimental Estimation of Lateral Forces (Review). VNIIZhT Bulletin. 2017. Vol. 76. No. 1. P. 10–18.
- [15] Verigo M.F., Gracheva L.O., Shafranovsky A.K., Anisimov P.S., Kreinis Z.L., Kobzeva Z.G. Lateral forces in straight sections of the track. VZIIT Proceedings. 1969. Issue. 42. P. 7–30.
- [16] Korolev K.P. Fitting steam locomotives into curved track sections. Proceedings of the Central Research Institute of the Ministry of Railways. Issue 37. Moscow: Transzheldorizdat, 1950. 224 p.
- [17] Ershkov O.P. Investigation of the stiffness of a railway track and its effect on the operation of rails in curved sections. Proceedings of the Central Research Institute of the Ministry of Railways. Issue 264. Moscow: Transzheldorizdat, 1963. S. 39–98.

- [18] Kreinis ZL, Fedorov IV, Shemelin Yu. N. Measurement of lateral forces in straight track sections based on rail deformations. VZIIT Proceedings. 1969. Issue. 42. S. 74–93.
- [19] Schlumpf U. Messungen mit Dehnungsmesstreifen bei den SBB. Technische Rundschau. Bern, 1955. No. 26. S. 35–41.
- [20] Weber H.H. Zur direkten Messung der Kräfte zwischen Rad und Schiene. Elektrische Bahnen. 1961. Nr. 5. S. 93–110.
- [21] GOST R 55050–2012. Railway rolling stock. Standards of permissible impact on the railway track and test methods. Moscow: Standartinform, 2013. 15 p.
- [22] Shevchenko D.V., Savushkin R.A., Kuzminsky Ya. O., Kuklin T.S., Rudakova E.A., Orlova A.M. Development of new methods for determining the force factors of the impact of rolling stock on the track. Railway engineering. 2018. No. 1 (41). S. 38–51.
- [23] Kossov V.S., Gapanovich V.A., Lunin A.A., Spirov A.V., Ilyin, I.E. Golubyatnikov A.V. On determining lateral forces in conditions of heavy traffic. Railway transport. 2018. No. 5. P. 46–51.
- [24] Kossov V.S., Lunin A.A. Determination of indicators of the impact of rolling stock on the railway track using the “RZD-2016” method. Materials of the XII Intern. Scientific and technical conference “Rolling stock of the XXI century: ideas, requirements, projects”. Saint Petersburg: PGUPS, 2017. S. 123–126.
- [25] Pat. 1794740 USSR: IPC B61K 9/08 (2006.01). Device for determining the pressure of the wheel on the rail / G.F. Agafonov, E.I. Danilenko, A.V. Grachev, L.N. Frolov, V.M. Romanov. No. 4784975/11; wilted. 01/22/1990; publ. 02/15/1993; bul. No. 6. 7 p.
- [26] Danilenko EI, Frolov LN, Romanov VM, Grachev A.B., Moras E. The influence of vertical load when measuring horizontal forces on the way. VNIIZhT Bulletin. 1979. No. 1. P. 41–44.
- [27] Pat. 2623665 Russian Federation: IPC G01L 5/16 (2006.01). Method of measuring three components of the load in the section of a rail in contact with a wheel of a railway rolling stock / V.S. Kossov, N.F. Krasnyukov, A.A. Lunin, V. A. Gapanovich; applicant and patentee of JSC Russian Railways. No. 2016119588; wilted. 05/20/2016; publ. 06/28/2017; bul. No. 19. 15 p.
- [28] Ahlbeck D.R., Harrison H.D. Technique for measuring wheel/rail forces with trackside instrumentation. ASME Winter Annual Meeting. Atlanta, Georgia, 1977. Rpt. # 77-WA / RT-9.
- [29] Harrison H.D., Ahlbeck D.R. Development and evaluation of wayside wheel/rail load measurement techniques. Proceedings international conference on wheel/rail load and displacement measurement techniques. Cambridge, Massachusetts, USA, 1981. P. 8–1 / 8–20.
- [30] Moreau A. La verification de la sécurité contre le déraillement sur la voie spécialisée de Villeneuve-Saint-Georges. Revue Générale des Chemins de Fer. France. 1987. Avril 2. P. 25–32.
- [31] Bocciolini L., Bracciali A., Benedetto L. Di, Mastandrea R., Piccioli F. Wayside measurement of lateral and vertical wheel / rail forces for rolling stock homologation. Proceedings of the 2nd International Conference on Railway Technology: Research, Development and Maintenance. Ed. by J. Pombo. Stirlingshire, Scotland: Civil-Comp Press, 2014. P. 1–23.
- [32] Cortis D., Bruner M., Malavasi G. Decoupling of wheel-rail lateral contact forces from wayside measurements. Transport Infrastructure and Systems:



Proceedings of the AIIT International Congress on Transport Infrastructure and Systems. CRC Press, 2017. P. 79–86.

[33] Li Y.F., Liu J.X., Lin J.H. Wheel-rail lateral force continuous measurement based on rail web bending moment difference method. *Applied Mechanics and Materials*. 2011. Vol. 105–107. P. 755–759.

[34] Cortis D., Giulianelli S., Malavasi G., Rossi S. Self-diagnosis method for checking the wayside systems for wheel-rail vertical load measurement. *Transport Problems*. 2017. Vol. 12. Iss. 4. P. 91–100.

[35] Feng Yu, Hendry M.T. A new strain gauge configuration on the rail web decoupled the wheel/rail lateral contact force from wayside measurement. *Proceedings of the IMechE, Part F: Journal of Rail and Rapid Transit*. 2019. Vol. 233. Iss. 9. P. 951–960.

[36] Milković D., Simić G., Jakovljević Ž., Tanasković J., Lučanin V. Wayside system for wheel/ rail contact forces measurements. *Measurement*. 2013. Vol. 46. Iss. 9. P. 3308–3318.

[37] Molatefi H., Mozafari H. Analysis of a new method for vertical load measurement in the barycenter of the rail web by using FEM. *Measurement*. 2013. Vol. 46. Iss. 8. P. 2313–2323.

[38] Bracciali A., Folgarait P. New sensor for lateral and vertical wheel-rail forces measurements. *Railway Engineering Conference. Railway Engineering*. 2004. P. 1–7.

[39] Bracciali A., Ciuffi R., Piccioli F. Progetto e validazione di un sensore estensimetrico multifunzione per il binario ferroviario. *Proceedings of the XXX Convegno Nazionale AIAS, Alghero (SS), Italy*, 2001. P. 901–912.

[40] Catalini R., Pacciani S., Pagliari M. Sistema di rilevamento del carico

dinamico (RICAD) trasmesso alla traversa dai treni in transito sul binario. *Ingegneria Ferroviaria*. 2003. Vol. 58. No. 9. P. 823–829.

[41] Delprete C., Rosso C. An easy instrument and a methodology for monitoring and diagnosing a rail. *Mechanical Systems and Signal Processing*. 2009. Vol. 23. Iss. 3. P. 940–956.

[42] Boronenko Yu. P., Rahimov R.V., Grigoriev R. Yu., Popov V.V. Analysis of methods for measuring the force effect of rolling stock on the track and the wheel control systems when the train is moving. *Bulletin of the Petersburg University of Railways*. Saint Petersburg: PGUPS, 2020. Vol. 17. Issue. 3. P. 324–344.

[43] GOST 8161–75. Railway rails of the R65 type. Design and dimensions. Moscow: Standards Publishing House, 1975. 9 p.

[44] Boronenko Yu. P., Rahimov R.V., Petrov A.A. Piecewise continuous force measurement between the wheel and rail shear stress in two rail sections. *Transport of the Russian Federation*. 2018. No. 3 (76). P. 58–64.

[45] Rahimov R.V. Loading of carriage running gears and tracks and substantiation of the possibility of increasing axle loads on the railways of the Republic of Uzbekistan: dis. ... doct. Tech. Sciences: 05.22.07. Saint Petersburg, 2020. 366 p.

[46] Rahimov R.V., Petrov A.A. Accuracy test for restoration of vertical loads from the wheel on the rail by stresses in two cross-sections of a rail on the test stand. *Transport of the Russian Federation*. 2018. No. 4 (77). P. 55–58.

[47] Rahimov R.V., Zhitkov Yu. B., Petrov A.A. Experimental determination of loads from a wheel on a rail by measured stresses in two rail

sections. Materials of the XIII International Scientific and Technical Conference “Rolling Stock of the XXI Century: Ideas, Requirements, Projects”. Saint Petersburg: PGUPS, 2018. P. 156–161.

[48] Boronenko Yu. P., Rahimov R.V., Sergeev D.A., Tsyganskaya L.V., Romanova A.A. Approbation of a new method for measuring vertical loading from wheel to rail. *Transport of the Russian Federation*. 2019. No. 1 (80). P. 56–59.

[49] Boronenko Yu. P., Rahimov R.V., Sergeev D.A. Refined measurement of vertical dynamic load from wheels on rails. *Proceedings of the National Scientific and Practical Conference “The Way of the XXI Century”*. Saint Petersburg: PGUPS, 2019, pp. 67–73.

[50] Boronenko Yu. P., Rahimov R.V., Lafta W.M., Dmitriev S.V., Belyankin A. V., Sergeev D.A. Continuous monitoring of the wheel-rail contact vertical forces using a variable measurement scale. *Proceedings of the 2020 Joint Rail Conference (JRC2020)*. St. Louis, Missouri, USA. April 20–22, 2020. JRC2020–8067, V001T13A006. ASME. P. 1–3.

[51] Boronenko Yu. P., Rahimov R.V. Measuring side loading from wheels to rails. *Transport of the Russian Federation*. 2019. No. 4 (83). P. 45–50.

[52] Boronenko Yu. P., Rahimov R.V. Experimental determination of lateral loads from wheel-rail interaction. *Transport of the Russian Federation*. 2019. No. 6 (85). S. 50–53.

[53] Boronenko Yu. P., Rahimov R.V., Lafta W.M. Develop a new approach measuring the wheel/rail interaction loads. *Proceedings of the 2021 Joint Rail Conference (JRC2021)*. Virtual, Online. April 20–21, 2021. JRC2021–58471, V001T10A004. ASME. P. 1–8.

[54] Pat. RU 2709704 C1 Russian Federation: IPC G01G 19/04 (2006.01), G01B 7/14 (2006.01). Method for measuring the vertical load from a wheel on a rail and a device for its implementation / Yu. P. Boronenko, A. S. Dauksha, R.V. Rahimov; applicant and patentee of JSC NVC Vagony. No. 2018140938; wilted. 11/21/2018; publ. 12/19/2019; bul. No. 35.14 p.

[55] Pat. R.U. 2720188C1 Russian Federation: IPC G01L 1/22 (2006.01). Method for measuring lateral forces acting from a wheel on a rail, and a device for its implementation / Yu. P. Boronenko, R.V. Rahimov, A.S. Dauksha; applicant and patentee of JSC NVC Vagony. No. 2019114559; wilted. 05/13/2019; publ. 04/27/2020; bul. No. 12.11 p.

[56] Boronenko Yu. P., Povolotskaia G. A., Rahimov R.V., Zhitkov Yu. B. Diagnostics of freight cars using on-track measurements. *Advances in Dynamics of Vehicles on Roads and Tracks. Proceedings of the 26th Symposium of the International Association of Vehicle System Dynamics (IAVSD 2019)*. Lecture Notes in Mechanical Engineering, August 12–16, 2019. Gothenburg, Sweden: Springer, Cham, 2020. P. 164–169.

[57] Pat. RU 2708693 C1 Russian Federation: IPC G01M 17/10 (2006.01). Device and method for detecting wheel defects of railway vehicles in motion / Yu. P. Boronenko, Yu. B. Zhitkov, R.V. Rahimov, G.A. Povolotskaya; applicant and patentee of JSC NVC Vagony. No. 2019103561; wilted. 02/08/2019; publ. 12/11/2019; bul. No. 35. 14 p.